AGU PUBLICATIONS

JGR

Journal of Geophysical Research: Atmospheres

RESEARCH ARTICLE
10.1002/2014JD022216

Key Points:
- Field evidence to support emissivity diurnal variations is presented
- AIRS emissivities are found not as good as MODIS using the field measurements
- The UWIREMIS takes advantages of both the high spatial and spectral resolution

Correspondence to:
Y. Zhang,
zhangyong@cma.gov.cn

Citation:
Zhang, Y., Z. Li, and J. Li (2014), Comparisons of emissivity observations from satellites and the ground at the CRCS Dunhuang Gobi site, *J. Geophys. Res. Atmos.*, *119*, doi:10.1002/2014JD022216.

Received 26 JUN 2014
Accepted 22 OCT 2014
Accepted article online 27 OCT 2014

Comparisons of emissivity observations from satellites and the ground at the CRCS Dunhuang Gobi site

Yong Zhang[1], Zhenglong Li[2], and Jun Li[2]

[1]National Meteorological Satellite Center, China Meteorological Administration, Beijing, China, [2]Cooperative Institute for Meteorological Satellite Studies, University of Wisconsin-Madison, Madison, Wisconsin, USA

Abstract Two sets of field-measured hyperspectral resolution infrared (IR) emissivity spectra were taken from the China Radiometric Calibration Sites (CRCS) Dunhuang site in China, with one representing daytime and the other representing nighttime. Comparisons of the two sets show that the daytime emissivity is smaller than the nighttime emissivity in almost the entire spectrum between 7.5 and 14 μm, strong field evidence to support emissivity diurnal variations, which have been reported in previous studies using satellite observations. These emissivities are used as a reference to evaluate three different emissivity products from the same site: the Atmospheric Infrared Sounder (AIRS) operational emissivity products, the Moderate Resolution Imaging Spectroradiometer (MODIS) operational emissivity products, and the University of Wisconsin-Madison Hyperspectral Resolution IR emissivity (UWIREMIS) database. The AIRS emissivity does not agree as well with the field measurements when compared to that from MODIS and the UWIREMIS despite the fact that AIRS is hyperspectral; the likely cause for the disagreement is cloud contamination due to AIRS' large footprint. MODIS has the advantage of high spatial resolution and visible/near-infrared channels to help the cloud mask and is therefore less affected by cloud contamination. The V4.1 MODIS emissivity agrees better with the field measurement than the UWIREMIS, while the V5 does not do as well. The UWIREMIS emissivity, on the other hand, has the advantage of hyperspectral resolution, which makes it more useful for applications. The temporal analysis of the three satellite-based emissivity products is also presented.

1. Introduction

With the rapid development of remote sensing technology, a large number of satellites with a high-performance thermal infrared (IR) detection capability have been launched into space. In China, to calibrate satellite infrared instruments, the in-orbit field calibration is used. Usually, this technique uses plateau lake sites with a high altitude, a dry and clean atmosphere with few aerosol particulates, less human disturbance, uniform temperature distribution, and that can result in high calibration accuracy, such as Lake Qinghai [*Zhang et al*., 2013] and Lake Titicaca [*Wan et al*., 2002]. However, these lakes often have very cold water surface temperatures, colder than most targets that satellites observe. As a result, the in-orbit field calibration using these lakes only ensures the calibration accuracy in the low end of the sensors' dynamic range. China has established two instrumented national radiometric calibration fields, called China Radiometric Calibration Sites (CRCS), for the absolute radiometric calibration of sensors [*Zhang et al*., 2009a]: a land surface site at Dunhuang Gobi [*Hu et al*., 2010] and a water surface site at Lake Qinghai [*Zhang et al*., 2013]. A number of instruments are deployed at these sites to gain accurate knowledge about atmospheric and Earth surface conditions [*Hu et al*., 2010; *Zhang et al*., 2009a; *Zhao et al*., 2003], which are needed to calibrate satellite instruments. Use of the CRCS Dunhuang site to calibrate satellite IR sensors greatly enhances the in-orbit field radiometric calibration method due to its high land surface temperature.

IR land surface emissivity (LSE) is one of the parameters measured accurately at the two sites. LSE is a key physical parameter to describe the IR radiation characteristics of the Earth's surface. It is defined as the ratio of the energy emitted by the land surface to that emitted by a blackbody at the same temperature and wavelength. As emissivity depends on wavelength, it is referred to as spectral emissivity. LSE substantially varies with viewing angle [*Rees and James*, 1992], vegetation, soil moisture, composition, and roughness [*Nerry et al*., 1988; *Salisbury and Aria*, 1992; *Hulley et al*., 2010], with typical values between 0.65 and 1.0 in the thermal IR (TIR) range. Lower values are observed over arid deserts, mainly consisting of quartz, in the two Reststrahlen bands around 4 and 8.5 μm, whereas an LSE close to 1 characterizes dense vegetation, water, or ice-covered surfaces [*Capelle et al*., 2012].

Studies [*Wan et al*., 1999, 2002; *Zhang et al*., 2005] have shown that uncertainty in LSE is one of the major sources of uncertainties in sensors' in-orbit absolute radiometric calibration and validation. LSE errors greatly affect the simulated brightness temperature, especially for window bands. For example, *Wan et al*. [1999] found that the effect of uncertainties in snow surface emissivity in the 10.975 μm band (less than 0.005) on the calculated TOA brightness temperature (BT) is around 0.30 K. This effect means that a minor LSE error of 0.005 could lead to a systematic calibration bias of 0.30 K. It is therefore extremely important for LSE to be as accurate as possible when it comes to the sensors' calibration and validation.

Accurate LSE is also needed for many other applications in satellite meteorology. The accuracy of LSE plays an important role in the inversion of land surface temperature (LST). Studies have shown that for a surface of 300 K, an emissivity error of 0.5% at 11 μm is equivalent to a surface temperature error of 0.3 K [*Galve et al*., 2008], and an error of 1.5% at 8.6 μm (this band typically has a much larger error than the split windows) may lead to a surface temperature error of approximately 1 K [*Hulley and Hook*, 2009a]. Similar impact studies can be found in *Zhang* [1999]. LSE accuracy is also critical for assimilating IR radiances in models over land [*Le Marshall et al*., 2006]; without an accurate LSE, the assimilation system may not take full advantage of IR surface channels, which contain important information about the lower atmosphere and Earth surface. Other applications that require accurate emissivity include, but are not limited to, atmospheric temperature and moisture sounding retrievals [*Li et al*., 2008, 2009], cloud top pressure retrievals [*Menzel et al*., 2008; *Li et al*., 2005], radiation budget [*Lee et al*., 2007], trace gas retrievals [*Clerbaux et al*., 2003; *Ho et al*., 2005], and dust and aerosol property retrievals [*Zhang et al*., 2006; *Li et al*., 2007a].

In recent years, whether it is in the lab or in the field, many technologies and methodologies have been developed to measure LSE. Laboratory-measured LSE is conducted in controlled laboratory conditions with soil samples taken from selected sites. While they are very accurate, they are often limited for satellite remote sensing applications due to the representativeness of the samples. Emissivity is not only dependent on the composition of the surface materials but also related to the state of the surface structures (roughness, etc.) and physical properties (dielectric constant, moisture content, temperature, etc.); surface emissivity also varies with wavelength (λ), zenith angle (θ), and other measuring conditions [*Zhao et al*., 2003]. Field-measured emissivity is conducted with a series of instruments to measure the surface and atmospheric conditions, which are used to overcome the difficulty in separating the surface signal from the atmosphere as well as separating the LSE signal from the LST. The representativeness of the area depends on the homogeneousness of the site. *Nerry et al*. [1990], *Hook and Gabell* [1992], *Salisbury and Aria* [1992], and *Rubio et al*. [1997] carried out numerous field experiments to measure soil TIR emissivity spectra. In China, scientists have also carried out many experiments to measure emissivity in the field; *Zhang and Tian* [1981] and *Zhang et al*. [2009a, 2009b] have used different methods and retrieval algorithms to measure the field emissivity of different surface types.

Satellite-measured emissivity has advantages compared to laboratory and field measurements. It is the most realistic way to obtain large spatial coverage with adequate spatial resolution, both of which are important for applications in satellite meteorology. Over the years, many LSE retrieval methods using satellite measurements have been developed [*Wan and Li*, 1997; *Seemann et al*., 2008; *Ruston et al*., 2008; *Li et al*., 2007b; *Zhou et al*., 2008; *Li and Li*, 2008; *Gillespie et al*., 1999; *Watson*, 1992; *Faysash and Smith*, 1999, 2000; *Peres and Dacamara*, 2004; *Rodger et al*., 2005; *Morgan*, 2005; *Li et al*., 2011]. Since the retrieval of LSE using satellite data is nonlinear and ill posed [*Li et al*., 2011], constraints or additional information are needed to help solve the inverse problem. The constraint could be a maximum value of LSE for one channel, the emissivity spectral shape or contrast, or other known information. Additional information, such as multiple observations, may also help solve the inverse problem. In the MODIS day/night algorithm [*Wan and Li*, 1997], a pair of day/night MODIS radiance observations is used to retrieve the same day/night emissivity; this process introduces only one additional unknown LST while doubling the number of observations. The GOES-R (next generation of the Geostationary Operational Environmental Satellite) Advanced Baseline Imager [*Schmit et al*., 2005] LSE algorithm [*Li et al*., 2011] takes advantage of the high temporal resolution from geostationary satellites and retrieves LSE using radiance observations from three time steps; this algorithm introduces only two additional unknown LSTs while tripling the number of observations for solving LST and LSE simultaneously. High spectral resolution IR sounders, such as Atmospheric Infrared Sounder (AIRS) onboard NASA's EOS Aqua [*Chahine et al*., 2006], the Infrared Atmospheric Sounding Interferometer (IASI) onboard Metop-A and Metop-B [*Hilton et al*., 2012] and the Cross-track Infrared Sounder on board the Suomi National Polar-Orbiting Partnership [*Han et al*., 2013], with thousands of spectral channels, offer improved

resolving power of the emissivity spectrum. The hyperspectral emissivity spectrum can be represented with a limited number of eigenvectors derived from a laboratory-measured hyperspectral emissivity database. This greatly reduces the number of unknowns in the inverse problem. With a physical iterative approach or a multivariate regression model, a hyperspectral emissivity spectrum can be retrieved simultaneously along with temperature and moisture soundings, as well as surface skin temperature from a hyperspectral IR radiance spectrum [*Li et al*., 2007b; *Li and Li*, 2008; *Zhou et al*., 2008; *Susskind et al*., 2003]. Each of these algorithms has its own advantages as well as limitations. *Z. L. Li et al*. [2012] reviewed most of the LSE retrieval methods and provided insights for further improvements. As far as a practical implementation for numerical weather prediction purposes, the UK Met Office has established an effective method [*Pavelin and Candy*, 2014] to analyze the LSE spectrum in order to assimilate land sensitive IASI radiances. Their method is also based on a limited number of eigenvectors, and positive impacts are observed especially in near-surface temperature and midtropospheric water vapor measurements.

Validation of satellite-measured emissivity is as difficult as the retrieval. The major difficulty is the availability of accurate emissivity data as a reference. Highly accurate laboratory and field measurements have been widely used to validate satellite-measured emissivity. For example, *Hulley and Hook* [2009b] analyzed the temporal and spatial variations of the MOD11 LST/LSE product for Versions 4, 4.1, and 5 and validated each product with laboratory emissivity measurements of sand samples collected from the Namib Desert in Namibia. *Dong et al*. [2013] performed the field validation of the global land surface satellite broadband emissivity database using pseudo-invariant sand dune sites in northern China. However, this technique only works over a limited homogeneous area of the Earth's surface. Alternatively, many studies seek intercomparison of various satellite measurements to gain some knowledge of the emissivity quality. *Sobrino et al*. [2001] compared LSE computed using four algorithms from National Oceanic and Atmospheric Administration (NOAA) data. *Jacob et al*. [2004] compared the LSE and radiometric temperatures derived from MODIS and Advanced Spaceborne Thermal Emission and Reflection Radiometer ASTER sensors. *Schmugge and Ogawa* [2006] validated the emissivity estimated from ASTER and MODIS data.

This study continues the efforts to compare and validate emissivity. Specifically, the highly accurate in situ emissivity measurements at CRCS Dunhuang Gobi are used to compare with other satellite-measured emissivity products, including AIRS, MODIS, as well as the UWIREMIS emissivity database. These three emissivity databases are chosen because they are operational products or based on operational products. The uniqueness of the in situ emissivity at CRCS Dunhuang Gobi is that measurements are available during both the day (around 3 P.M. local time) and night (around 5 A.M. local time) so that emissivity diurnal variation can be examined. According to *Z. Li et al*. [2012], LSE in the Sahara Desert possesses a diurnal wave pattern variation with low values during daytime and high values during nighttime. These in situ measurements will be the first to support emissivity diurnal variations as demonstrated from satellite observations [*Z. Li et al*., 2012; *Masiello et al*., 2013]. All three satellite databases have global coverage with decent spatial resolutions. Intercomparisons of satellite emissivity products will also be conducted.

Section 2 provides a brief introduction of the CRCS Dunhuang Site. Section 3 describes the data used for comparisons in this study. Sections 4 and 5 present results, discussions, and conclusions.

2. CRCS Dunhuang Site

The CRCS Dunhuang site (40.1821°N, 94.3244°E) is located in the Gobi Desert in northwest China, about 35 km west of Dunhuang City, Gansu Province. Covering approximately 30 km × 30 km, the entire site is formed on a stable alluvial fan of the Danghe River (Figure 1) and its surface consists of cemented gravel without vegetation (Figure 2). Dunhuang was chosen as a CRCS site due to its extremely homogeneous surface conditions. The detailed characteristics of the CRCS Dunhuang Site are listed in Table 1. The central area (600 m × 600 m) of the site is designed for high spatial resolution visible/near-infrared (VIS/NIR) sensors such as the China-Brazil Earth Resources Satellite (CBERS) series. An extended large area (20 km × 20 km) is used for low spatial resolution sensors such as the Multichannel Visible and Infrared Scanning Radiometer, Visible and Infrared Radiometer, and Medium Resolution Spectral Imager on board the Fengyun-1 and 3 (FY-1/3) series of polar-orbiting satellites. It is also used for the field calibration of the VIS/NIR channels on Chinese geostationary weather satellites (Fengyun-2 or FY-2 series). Field calibration of the FY series of satellites has been conducted operationally since 2001 for only the VIS/NIR channels. Due to the lack of onboard VIS/NIR calibrators, the

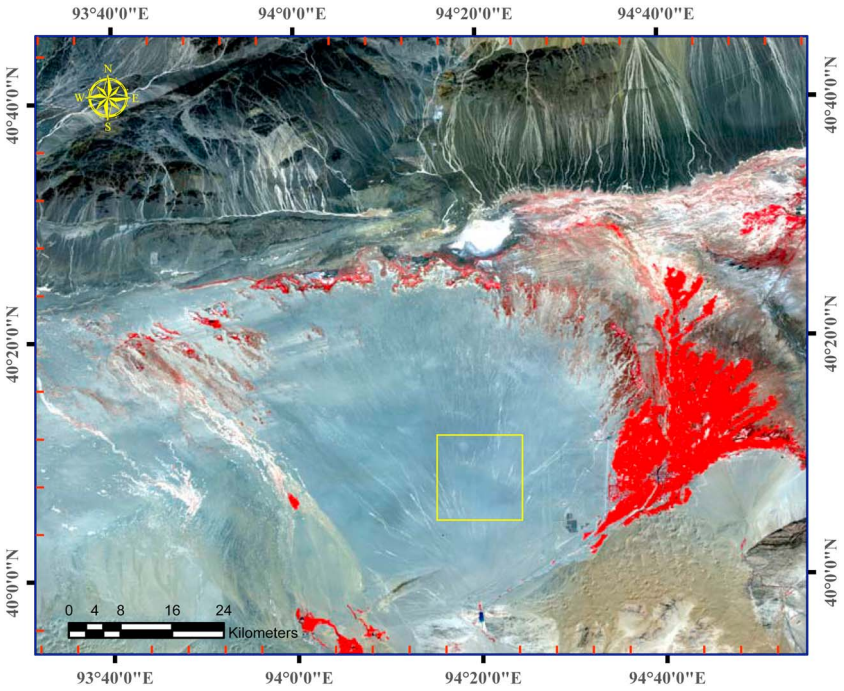

Figure 1. The false RGB color composite (R: 0.45–0.52 μm, G: 0.52–0.59 μm, and B: 0.77–0.89 μm) GF-1 Wide Field View (WFV) image with 16 m spatial resolution on 2 August 2013. The yellow square is the central area for the FY satellite series calibration. The red areas are vegetation-covered areas.

in-orbit field calibration based on the CRCS Dunhuang site is still the primary method for China's satellite sensors' VIS/NIR channels, such as the FY series satellites, Haiyang (HY) series of Ocean Satellites, Disaster and Environmental Monitoring Satellites (HJ), and CBERS series satellites. In recent years, the CRCS Dunhuang site has also been used for FY satellite IR channel field radiometric calibration [*Zhang*, 2012; *Zhang and Qi*, 2013].

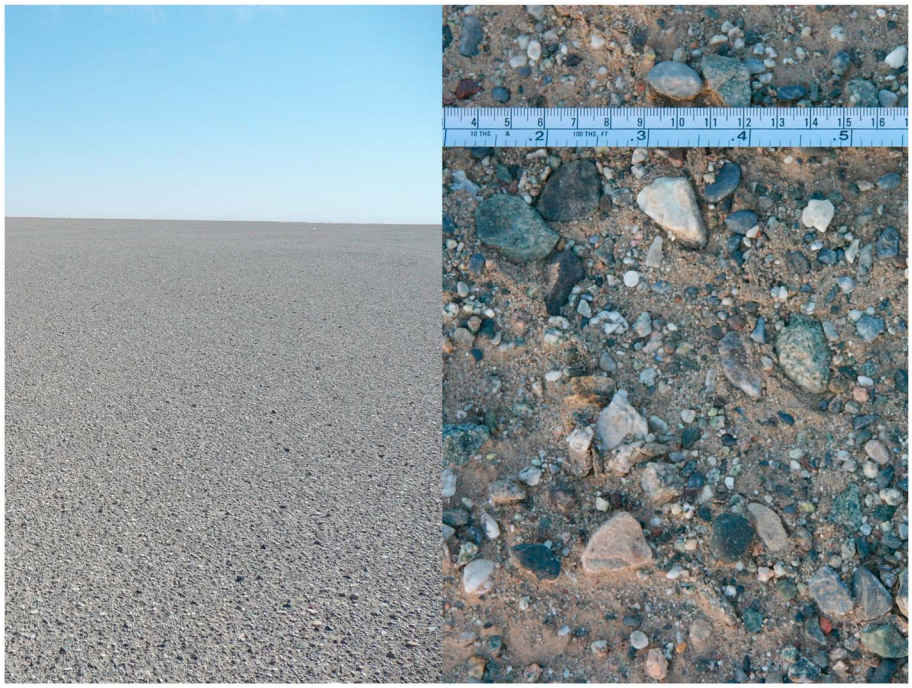

Figure 2. Photographs of the CRCS Dunhuang Gobi surface. This site consists of cemented gravel and lacks vegetation.

Table 1. Characteristics of the CRCS Dunhuang Site

Feature Parameters		CRCS Dunhuang Site
Location		Dunhuang City, Gansu Province, 40.1821°N, 94.3244°E
Altitude		1160 m
Area		30 km × 30 km
Surface feature		Gobi Desert without vegetation
Climate type		Dry continental climate
Averaged annual meteorological parameters	Surface pressure	887.6hpa
	Surface air temperature	9.5 °C
	Annual precipitation	34.1 mm
	Surface relative humidity	43.9%
	Annual sunshine time	3270 h
	Annual clear days	112.2 days
	Days with visibility greater than 10 km	288.2 days
Reflectivity in VIS/NIR channels		15%–30%

3. Data

To compare the CRCS Dunhuang Site Gobi surface emissivity data, different types of emissivity data were collected, compared, and analyzed, including field-measured high spectral emissivity and satellite-retrieved emissivities. Brief introductions of these data are shown below.

3.1. High Spectral Resolution Emissivity In Situ Measurements

The spectral emissivity data were measured in the field by *Zhang et al*. [2009a] with a set of instruments at the CRCS Dunhuang site. Based on the iterative spectrally smooth temperature/emissivity separation algorithm [*Ingram and Henry*, 2001], Dunhuang Gobi surface emissivity spectra were measured using a BOMEM MR154 Fourier transform spectroradiometer [*BOMEM Inc*, 1995] and Infrared Golden Board for both day and night. For the nighttime data, the measurements were taken for 11 valid repeats from 4 to 6 A.M. (GMT +8) on 1 August 2007, and eight valid repeats from 2 to 4 P.M. (GMT +8) on 12 October 2007 for daytime data. At the CRCS Dunhuang site, there is no vegetation; emissivity variations due to physical changes in the surface should be minimal; variations should be mostly caused by soil moisture content variation, which is highly related to LST. The mean LST from 4 to 6 A.M. (GMT +8) on 1 August is 284.5 K and 307.5 K from 2 to 4 P.M. (GMT +8) on 12 October 2007, which were also measured by the BOMEM MR154 Fourier transform spectroradiometer and Infrared Golden Board. The mean LST diurnal variation from these two sets of measurements is 23.0 K. This LST diurnal variation along with corresponding soil moisture changes should cause corresponding LSE variations. It is important to point out that this LST diurnal variation might be a slight underestimation of real LST diurnal variation for both dates; it is very likely that the daytime LST of 1 August is warmer than 307.5 K, and the nighttime LST of October 12 is colder than 284.5 K. The emissivity diurnal variations were first reported by *Z. Li et al*. [2012] and confirmed by *Masiello et al*. [2013]. These highly accurate measurements of emissivity spectra offer a great opportunity to examine satellite-measured emissivity during both day and night.

3.2. AIRS Retrieval Global Emissivity Data

The AIRS retrieval global emissivity data are from AIRS level-3 Version 5 and 6 Standard Products [*Tian et al*., 2013; *Susskind et al*., 2014]. The global 8 day and monthly averaged AIRS emissivity products in 1 by 1° grids are used in this study. Emissivity measurements of the ascending orbits are separated from those of the descending due to their different overpass times, with ascending orbits mainly in the early morning around 1:30 local time and descending orbits in the late afternoon around 13:30 local time. In this study, the satellite-measured emissivity data and the field measurements are collocated spatially and temporally for comparisons and analysis. Despite being a high spectral IR sounder, AIRS emissivity is only available at four spectral bands, 832, 961, 1203, and 2616 cm^{-1} or 12.02, 10.41, 8.31, and 3.82 μm.

3.3. Global MODIS Emissivity Science Product

The MODIS retrieval global emissivity data are from MODIS LST Products Collection-4.1 [*Wan and Li*, 1997] and 5 [*Wan*, 2008]. The MODIS LST/LSE science products are retrieved using the day/night algorithm, which uses a pair of day/night MODIS radiance observations and assumes that the emissivity does not

change during the 12 h while the LST changes. The daily LST/LSE products are used to generate the 8 day and monthly (MOD/MYD11) global gridded products. The MOD/MYD11 LST/LSE products have a spatial resolution of 0.05° in both latitude and longitude. In this paper, the emissivity data collocated with field-measured data in space and time in three MODIS window channels (channel 29 or 8.55 μm, channel 31 or 10.8 μm, and channel 32 or 12.02 μm) were used and compared. As of the writing of this manuscript, MODIS Collection 6 LSE/LST products [*Wan*, 2014] were not publicly available.

3.4. UW-Madison High Spectral Resolution IR Emissivity Database

The UWIREMIS database is a high spectral resolution (wave number resolution between 2 and 4 cm^{-1}) emissivity product with 416 wave numbers (from 3.6 to 14.3 μm) and a spatial resolution of 0.05° in both latitude and longitude. It is generated through two steps. In the first step, the University of Wisconsin (UW)-Madison baseline fit (BLF) emissivity database is derived using the MODIS LSE operational products, MOD11, as input. The baseline fit method [*Seemann et al*., 2008], based on a conceptual model developed from laboratory measurements of surface emissivity, was applied to fill in the spectral gaps between the six emissivity wavelengths available in MOD11. The six available MOD11 wavelengths span only three spectral regions (3.8–4, 8.6, and 11–12 μm), while the retrievals of atmospheric temperature and moisture from satellite IR sounder radiances require surface emissivity at higher spectral resolution and broader spectral coverage. Emissivity in the baseline fit database is available at 10 wavelengths (3.6, 4.3, 5.0, 5.8, 7.6, 8.3, 9.3, 10.8, 12.1, and 14.3 μm). These 10 wavelengths were chosen as hinge points to capture as much of the shape of the higher-resolution emissivity spectra as possible between 3.6 and 14.3 μm. In the second step, the UW High Spectral Resolution IR emissivity (UWIREMIS) algorithm [*Borbas et al*., 2007] was used to create high spectral resolution emissivity spectra from a combination of laboratory measurements of selected materials and the UW BLF global IR LSE database [*Seemann et al*., 2008]. The algorithm is based on a statistical regression: the first six eigenvectors of 123 selected high spectral resolution laboratory spectra were regressed against the 10 hinge points of the monthly UW BLF emissivity data. According to *Li et al*. [2010], the UWIREMIS emissivity has a comparable or slightly better quality than the operational MODIS LSE products over the Sahara Desert.

4. Results

In order to compare the LSE data of the CRCS Dunhuang Gobi obtained from different sources, four comparisons were conducted: (1) Comparisons between UWIREMIS and field-measured IR surface emissivity spectra: both of these measurements are hyperspectral, (2) comparisons between AIRS and MODIS channel emissivity data: both provide emissivity at limited channels but at the same observation time and angle, (3) comparisons between field-measured and satellite-retrieved LSE at MODIS spectral bands, and (4) long-term analysis of satellite-retrieved LSE at the CRCS Dunhuang Site. All the data are collocated spatially (nearest pixel with a distance less than the sensor's spatial resolution) and temporally (the field observation time falls in the satellite time range) with field-measured emissivity spectra. The location of the measured emissivity is 40.1375°N, 94.3208°E in the central area of the CRCS Dunhuang site. The times of the field measurements were in the early morning (around 5 A.M. local time) on 1 August and afternoon (around 3 P.M. local time) on 12 October 2007, representing night and day, respectively.

4.1. Comparisons Between UWIREMIS and Field-Measured IR Surface Emissivity Spectra

Among the four different types of measurements, the field measurements and UWIREMIS emissivity database are hyperspectral, allowing a comparison of them between 7.5 and 14 μm. This range is specially selected as there is less noise in the field measurements. Figure 3 shows the UWIREMIS emissivity and the field measurements for daytime on 12 October (Figure 3a) and the nighttime on 1 August 2007 (Figure 3b). In the quartz Reststrahlen bands around 8.55 μm, both measurements have low emissivity with a similar shape, indicating that both of them are capable of identifying quartz in the Earth's soil. These bands, located in the fundamental vibrational stretching modes in the IR range, often have high reflectance [*Hapke*, 1993] and low emissivity according to Kirchhoff's law of thermal radiation; they are extremely sensitive to the surface soil quartz contents. Soil at the CRCS Dunhuang Gobi site consists of cemented gravel with a high percentage of quartz without vegetation. Both measurements successfully identify and characterize the quartz signal and convert that to the right emissivity spectrum shape. In other spectral regions, the UWIREMIS measurements also show the right spectral shape, i.e., the drop in emissivity around 12.5 μm.

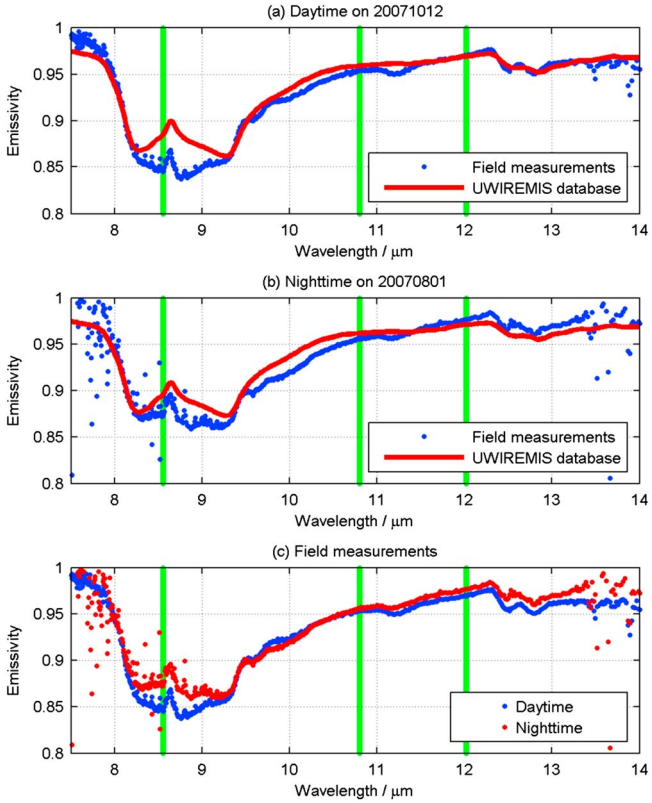

Figure 3. The Dunhuang Gobi surface emissivity spectra from (a) the daytime of field measurements and the UWIREMIS database, (b) the nighttime of the field measurements and the UWIREMIS database, and (c) the daytime and nighttime of the field measurements. The daytime measurement is the mean spectrum of eight repeated measurements from 2 to 4 P.M. on 12 October 2007, and the nighttime measurement is the mean spectrum of 11 repeated measurements from 4 to 6 A.M. on 1 August 2007. The UWIREMIS emissivities are the monthly products of October and August of 2007. Green lines denote the central wavelengths of MODIS 8.55, 10.80, and 12.02 μm.

Despite the similar shape, it is clear that there are substantial differences between the UWIREMIS emissivity and field measurements. In the quartz Reststrahlen bands around 8.55 μm, the UWIREMIS emissivities are larger than the field measurements for both day and night. The maximum difference in those bands is close to 0.05 for the daytime on 12 October 2007 and close to 0.025 for the nighttime on 1 August 2007. Notice that the random spikes are due to noisier field emissivity in the longwave CO_2 (greater than 13 μm) and water vapor bands (smaller than 8 μm); the spectral radiometer has more noise in the BTs at night when the target is colder than during the day. Quantitative comparisons show that the UWIREMIS database agrees with field measurements reasonably well. The mean difference is very small (0.0067) between UWIREMIS and the field measurements for daytime with a small standard deviation of 0.0144. The mean difference for nighttime is also very small (0.0018) with a standard deviation of 0.037. The larger standard deviation at nighttime is due to noisier field measurements.

Comparing the two field measurements in Figure 3c, the night field emissivities are larger than the day emissivities in almost the entire spectrum between 7.5 and 14 μm, suggesting a diurnal variation in LSE. To our knowledge, this is the first field/laboratory emissivity measurement directly showing LSE diurnal variations. LSE diurnal variations in a desert were first reported by *Z. Li et al.* [2012] using Spinning Enhanced Visible and Infrared Imager [*Schmetz et al.*, 2002], and *Masiello et al.* [2013] verified that using IASI. In desert areas without vegetation, soil moisture diurnal variation [*Agam and Berliner*, 2004] is believed to be the main reason for emissivity diurnal variation. Evidence that emissivity is affected by soil moisture can be found in *Mira et al.* [2007], *Ogawa et al.* [2006], *Hulley et al.* [2010], and *Sanchez et al.* [2011]. Without precipitation, the desert soil moisture may diurnally vary due to adsorption of water vapor by sand particles [*Jackson et al.*, 1997]. As mentioned in section 3.1, the mean LST is 284.5 K for nighttime on 1 August 2007 and 307.5 K for daytime on 12 October 2007. The higher LST during the day causes more evaporation and less adsorption of water vapor and thus less soil moisture content, which in turn reduces the LSE values.

An important weakness of the above analysis is the lack of information on the quality of the field measurements. To address that, an error analysis of the measured emissivity spectra was calculated. Figure 4 shows the spectra of the standard deviation of the measured emissivity for both daytime and nighttime. For the Reststrahlen band, the standard deviation is around 0.02 in the day and around 0.01 at night, smaller but still comparable to the diurnal variations shown in Figure 3. However, this does not mean that the field-measured emissivities are of poor quality. Figure 4 shows that the daytime has more emissivity variances than the nighttime. This is surprising because the spectroradiometer-measured radiances in the day should have smaller BT noises due to warmer targets. However, the variances shown in

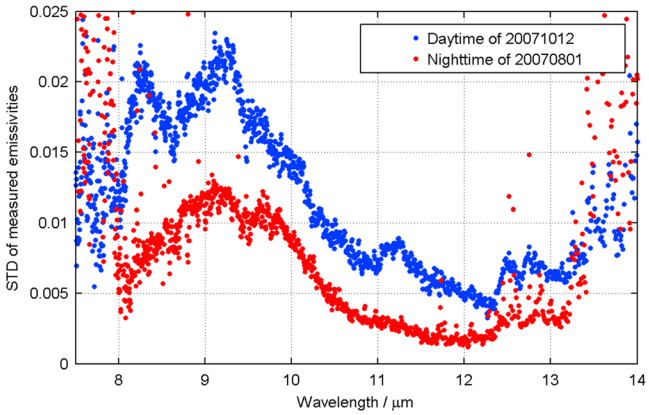

Figure 4. Error analysis of the field-measured emissivities for the daytime on 12 October 2007 (blue) and the nighttime on 1 August 2007 (red). The standard deviations (standard deviations) at each spectral band are calculated from the 8 and 11 repeated measurements for daytime and nighttime, respectively. The large variances with nicely tight patterns in window region (8–13 μm) are mostly caused by temporal variations of emissivities. The random and large variances in longwave CO2 (greater than 13 μm) and water vapor (smaller than 8 μm) are mostly caused by instrument random noise.

Figure 4 are not exclusively due to measurement noise. In fact, it is reasonable to believe that most of the variances in Figure 4 are caused by the temporal variations of measured emissivities. According to *Z. Li et al.* [2012], there are more emissivity temporal variations in the day than in the night because the LST has larger temporal variations in the day due to sun heating, which in turn affects the moisture adsorption by the sand particles. Besides, the random noises in the spectroradiometer radiances should also look random in the emissivity standard deviation spectra, like those in the longwave CO_2 (greater than 13 μm) and water vapor (smaller than 8 μm) bands. Most of the standard deviation spectra between 8 and 13 μm in Figure 4 have nicely tight patterns. It is therefore reasonable to believe that the field-measured emissivities are of good quality and can be used as a reference to study emissivity diurnal variations and satellite-derived emissivity products.

4.2. Comparisons Between Fields Measured and Satellite Retrieval Emissivity Data

Satellite sensors measure the outgoing radiation with a finite spectral bandwidth. Therefore, the channel emissivity is a weighted average expressed by the following:

$$\varepsilon_i = \frac{\int_{\lambda_1}^{\lambda_2} f_i(\lambda)\varepsilon(\lambda)\mathrm{d}\lambda}{\int_{\lambda_1}^{\lambda_2} f_i(\lambda)\ \mathrm{d}\lambda}$$

where $f_i(\lambda)$ is the spectral response function (SRF) of channel i, $\varepsilon(\lambda)$ is the spectral emissivity, λ_1 and λ_2 are the lower and upper boundaries of the wavelength of channel i, and ε_i is the channel emissivity. Figure 5 shows the SRFs of MODIS/Terra (MOD) and MODIS/Aqua (MYD) band 29 (8.55 μm), band 31 (10.8 μm), and band 32 (12.02 μm). Note that there are very small differences in SRFs between the two MODIS instruments. The resulting emissivity difference should also be very small.

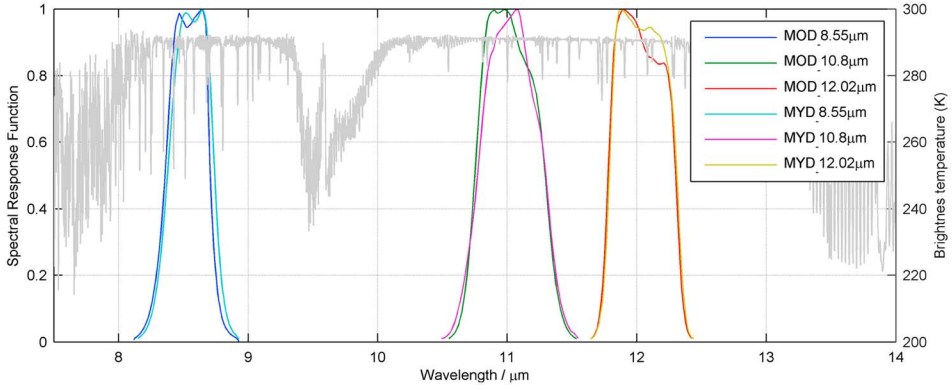

Figure 5. The spectral response functions of MODIS/Terra (MOD) and MODIS/Aqua (MYD) 8.55, 10.8, and 12.02 μm bands on top of a BT spectrum in gray line. Note that the three MODIS spectral bands are all in the window region.

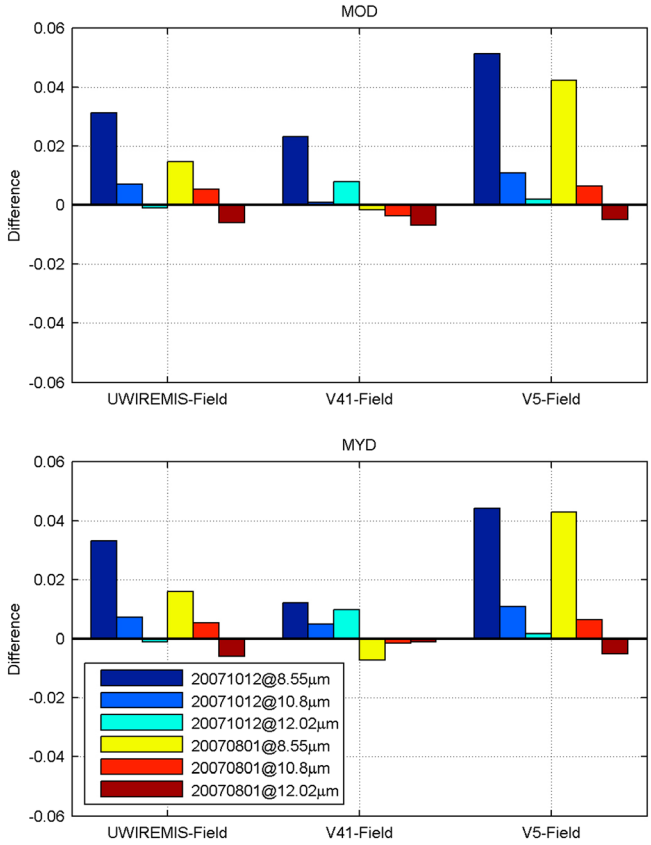

Figure 6. The emissivity differences between the UWIREMIS/MODIS and the field measurements at (top) MODIS/Terra (MOD) and (bottom) MODIS/Aqua (MYD) spectral bands. All hyperspectral emissivities are converted to MODIS spectral bands of 8.55, 10.8, and 12.02 μm using MODIS spectral response functions.

In order to validate the satellite retrieval emissivity data, all high spectral emissivity data, including UWIREMIS and field measurements data, are converted to MODIS channel emissivities using the MOD and MYD SRFs. Since UWIREMIS is only available monthly, only monthly measurements are studied. The field measurements are used as a reference. The results are shown in Figure 6. For the split window channels, all emissivity products show excellent agreement with the field measurements. For 8.55 μm, both MODIS V4.1 and the UWIREMIS show good agreement with the field measurements; the MODIS V5 emissivities, on the other hand, are 0.04 larger than the field measurements. The V4.1 MODIS operational emissivity products (both MOD and MYD) show a slightly better agreement with field measurements than the UWIREMIS. However, the UWIREMIS has the advantage of high spectral resolution while MODIS operational products are available only at limited spectral channels.

4.3. Comparisons Between AIRS and MODIS Channel Emissivity Data

Despite the high spectral resolution of radiance observations, AIRS level-3 emissivity is only available at four spectral channels, three of which (8.31, 10.41, and 12.02 μm) are very close to three MOD11/MYD11 spectral bands (8.55, 11.03, and 12.02 μm), allowing a direct comparison of them without spectral interpolation. In addition, both MODIS/Aqua and AIRS are from the same platform, thereby minimizing the complications caused by differences in observation time, angle, and locations. The comparison between MODIS and AIRS will provide insight into the tradeoff between spectral and spatial resolutions when resolving emissivity. Note that MODIS, with higher spatial resolution, allows better cloud detection. For MODIS products, Terra and Aqua satellites are separated because of different imaging times. And for AIRS products, descending and ascending orbits products are also separated for day and night imaging times. Since both MODIS and AIRS emissivity products are temporally averaged (8 day average from 29 July to 5 August or 9 to 16 October and monthly average from 1 to 31 August or 1 to 31 October), only weak temporal variations may be present when comparing emissivities from August to October.

Figure 7 shows the results. Overall, MODIS emissivities from different time periods, different versions, and different platforms are similar to each other, indicating the consistency of the MODIS LSE retrieval algorithm and the MODIS radiance observations. This is more evident for Version 4.1 than Version 5. Comparing the 8 day MODIS emissivities in Figures 7a and 7c, the 8.55 μm emissivities from 12 October 2007 is substantially smaller than 1 August 2007. This is also true for monthly MODIS emissivity products in Figures 7e and 7g. Considering the MODIS emissivity products in Figure 7 are all temporally averaged, the large temporal variations shown from MODIS Version 5 might indicate that the quality of the MODIS V5 emissivity is not as good as that from V4.1. Table 2 shows the statistics calculated using the field measurements as reference. All channels, versions, time periods (8 day and monthly) are put together to evaluate the overall agreement between the MODIS products and the field measurements. These results indicate that (1) the MODIS emissivity products (both

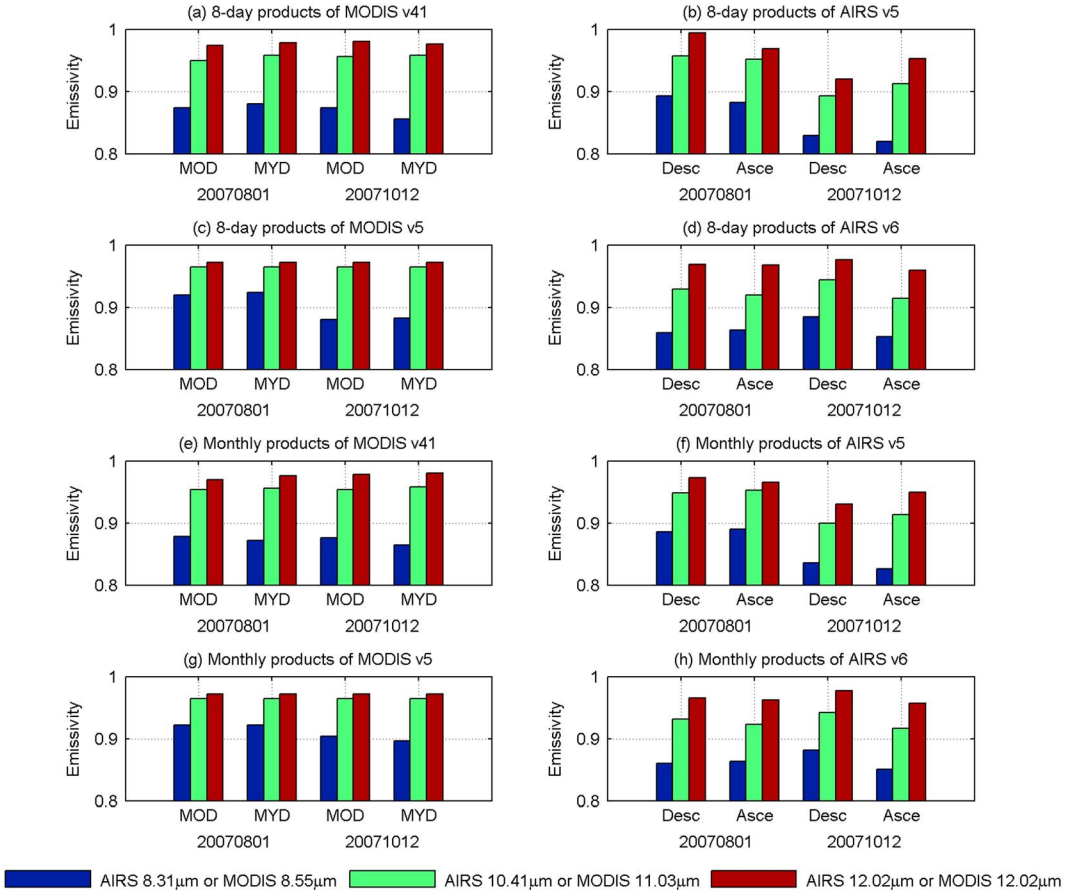

Figure 7. Satellite-retrieved emissivities from 1 August and 12 October 2007: (a, c, e, and g) from MODIS products and (b, d, f, and h) from AIRS products. Figures 7a–7d show 8 day products of AIRS/MODIS, and Figures 7e–7h show monthly products. MOD and MYD mean products from Terra/MODIS and Aqua/MODIS, respectively. Desc and Asce mean products from AIRS descending and ascending orbits, respectively.

versions) agree well with the field measurements and (2) V4.1 agrees with the field measurements better than V5. All the mean differences for V4.1 are smaller than 0.006 in absolute values. For V5, the split window channels have mean differences smaller than 0.009 in absolute values with channel 8.55 μm having a mean difference larger than 0.04. The standard deviations of differences are also very small for V4.1 (all smaller than 0.008), again indicating excellent agreement with field measurements. The standard deviation for 8.55 μm of V5 is 0.0185, which indicates good quality but not as good as that from V4.1. Channels 11.03 and 12.02 μm have zero standard deviations because the V5 day/night algorithm uses a classification-based emissivity scheme for the split window channels. These results are similar to those found in Africa by *Hulley and Hook* [2009b].

The quality of the AIRS emissivity products in Figure 7 appears to be mixed. Version 5 shows strong temporal variations for all three channels. In Figure 7b, the AIRS descending emissivities from 12 October 2007 are

Table 2. Statistics of the Differences Between Field Measurements and MODIS/AIRS Emissivity Products (MODIS/AIRS-Field), Which Include Day/Night and MYD/MOD

	Channels	MODIS_V41	MODIS_V5	AIRS_V5	AIRS_V6
Mean_Diff	8.31 μm for AIRS or 8.55 μm for MODIS	0.0059	0.0404	−0.0082	−0.0016
	10.41 μm for AIRS or 11.03 μm for MODIS	0.0001	0.0086	−0.0268	−0.0279
	12.02 μm for AIRS and MODIS	0.0029	−0.0016	−0.0169	−0.0068
SD	8.31 μm for AIRS or 8.55 μm for MODIS	0.0080	0.0185	0.0327	0.0124
	10.41 μm for AIRS or 11.03 μm for MODIS	0.0028	0.0000	0.0264	0.0113
	12.02 μm for AIRS and MODIS	0.0033	0.0000	0.0238	0.0072

much smaller than those from 1 August 2007 for all three channels; the differences for 10.41 and 12.02 μm are 0.0635 and 0.0742, respectively. While 8.31 μm may have substantial temporal variations due to surface condition variations at this site (the lack of vegetation), the variations from the two split window channels are not realistic. Similar temporal variations are observed from both the ascending and descending orbits and from both the 8 day and monthly products. These results indicate the possible poor quality of the AIRS V5 emissivity products. Version 6, on the other hand, shows much more reasonably stable results. For 8 day AIRS emissivities in Figure 7d, 8.31 μm sees an increase of 0.0249 from 1 August 2007 to 12 October 2007 from the descending orbits and a decrease of 0.0107 from the ascending orbits. Similar temporal variations are presented in the monthly AIRS emissivity products in Figure 7h. The split window channels also show slight temporal variations, which are within a reasonable range. The statistics in Table 2 also show better agreement with the field measurements from AIRS V6 than from V5. The mean differences between the two versions are similar to each other, but the standard deviations from V6 show much better agreement with the field measurements; the 8.31 μm has the largest standard deviation of 0.0124, which is much smaller than the smallest standard deviation from V5 (0.0238 from 12.02 μm). These results indicate a significant improvement of AIRS V6 emissivity product over V5.

However, in Table 2, comparing the statistics from AIRS V6 emissivity with MODIS V4.1, it is clear that MODIS agrees with the field measurements much better than AIRS. This result is somewhat unexpected considering AIRS' high resolving power from its thousands of channels. As a matter of fact, previous evaluation [*Li et al.*, 2010] has shown that the hyperspectral instruments (AIRS and IASI) do not necessarily lead to better emissivity compared with broadband imagers. However, this does not diminish the value of hyperspectral IR sounders for two reasons. First, the major problem with hyperspectral emissivity retrieval is cloud contamination. The chance of a footprint to be absolutely clear is related to its size. The larger the size, the lower the chance that the footprint is clear. The AIRS footprint size is 13.5 km at nadir. At this size, the chance of a footprint to be absolutely clear is around 10% [*Huang and Smith*, 2004]. With more cloud-contaminated footprints, cloud detection is much more challenging for AIRS. Any undetected clouds have negative impacts on the emissivity retrieval. Second, hyperspectral IR sounders offer better opportunities than individual channels to resolve the emissivity spectrum. Although the operational AIRS emissivity products are only available on limited channels, full spectral emissivity could be retrieved from hyperspectral IR sounder radiances as demonstrated by *Li et al.* [2007b] and *Zhou et al.* [2008] for AIRS and by *Zhou et al.* [2008] for IASI.

4.4. Long-Term Analysis of Surface IR Emissivity Data at CRCS Dunhuang Gobi

Emissivity usually does not change dramatically with time where there is little precipitation and vegetation, as is the case at the Dunhuang site. Though to some extent, it varies with soil moisture. For temporally averaged emissivity, there should not be large temporal variations. The emissivity time series should provide some indication about the quality of the emissivity products. Figure 8 shows the AIRS emissivity products at three wavelengths—8.31, 10.41, and 12.02 μm—separated between day and night during 2007, together with six field measurements at the same wavelengths and day/night. For 8 day products, AIRS V5 emissivity (Figure 8a) shows very strong temporal variations for all three channels for both day and night. Looking at the maximum temporal variation (MTV), the difference between the maximum and the minimum during 1 year, the MTVs for AIRS V5 8 day emissivity products are 0.1958, 0.1880, and 0.1440 for 8.31, 10.41, and 12.02 μm, respectively. For a desert without vegetation, these temporal variations are too large considering that they are the 8 day averaged emissivity. Notice that some emissivities are even larger than 1. These results are consistent with *Li et al.* [2010] where they found the quality of the AIRS V5 emissivity to be quite low. V6, on the other hand, shows significantly less temporal variation (see Figure 8b). The V6 MTVs are 0.0576, 0.0791, and 0.0356 for 8.31, 10.41, and 12.02 μm respectively, which are much smaller and more reasonable than those from V5. It is interesting that for all three channels, the nighttime emissivity is almost always smaller than the daytime, in stark contrast to the emissivity diurnal variation shown in Figure 3 in section 4.1 and in *Z. Li et al.* [2012] and *Masiello et al.* [2013]. The 10.41 μm appears to have the largest day/night differences among the three channels. This is again not consistent with Figure 3 and *Z. Li et al.* [2012] and *Masiello et al.* [2013], where they found that the quartz Reststrahlen bands around 8.55 μm have a larger diurnal variation than the split window channels. These results indicate that the AIRS V6 emissivity may not be able to capture the emissivity diurnal variations well at this site.

With more samples to average, the monthly products in Figures 8c and 8d show much smoother temporal variations than the 8 day. However, the seasonal variations in AIRS V5 monthly emissivity products are still

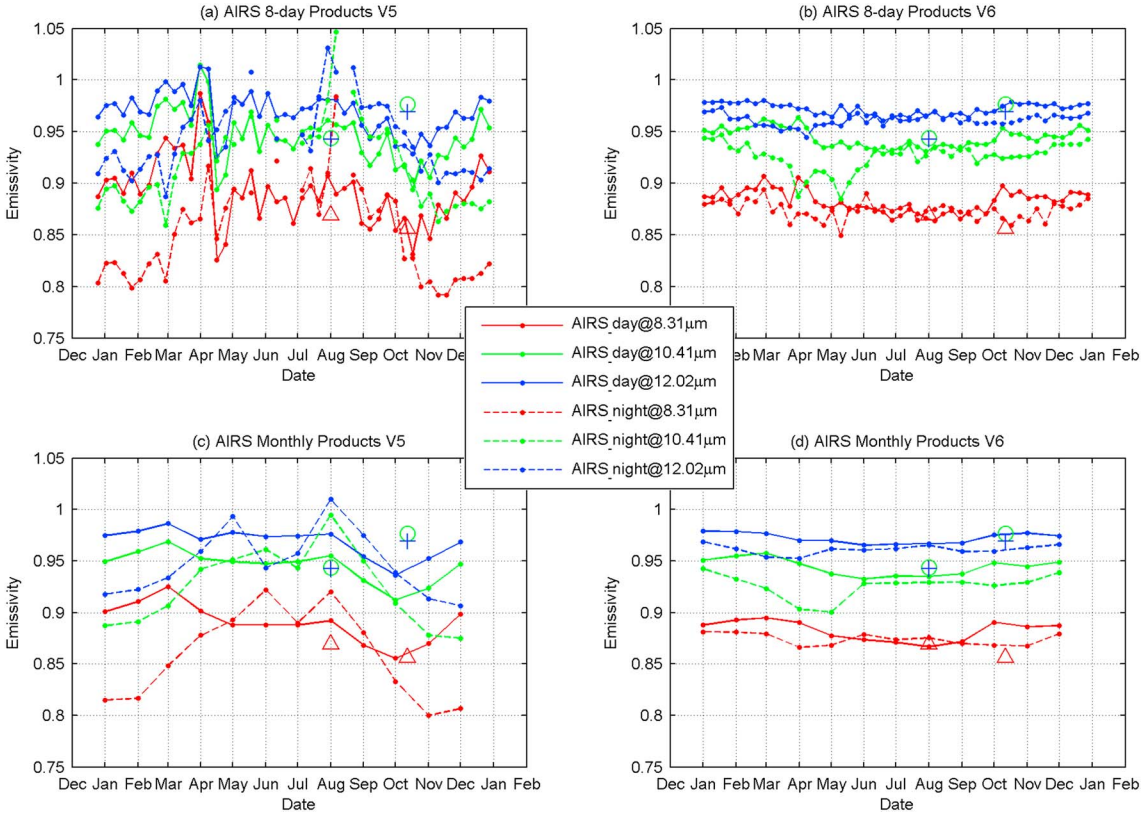

Figure 8. The time series of the AIRS (a, c) Version 5 and (b, d) Version 6, 8 day (Figures 8a and 8b) and monthly (Figures 8c and 8d) emissivity products at the CRCS Dunhuang site for all of 2007, together with field measurements. For AIRS products, the daytime data are from descending orbits (solid line with dots) and the nighttime data are from ascending orbits (dashed lines with dots). For field measurements, the daytime data are from 12 October and the nighttime data are from 1 August 2007 (triangles for 8.31 μm, circles for 10.41 μm, and plus for 12.02 μm).

strong; especially during nighttime, all three channels show that emissivity has higher values during warm seasons than cold seasons. The MTVs for AIRS V5 monthly emissivity products are 0.1255, 0.1196, and 0.1030 for 8.31, 10.41, and 12.02 μm, respectively. No observations have shown similar emissivity seasonal variations at the Dunhuang site. Similar to the V6 8 day products, the V6 monthly products show less significant temporal variations. However, the nighttime emissivity is still smaller than that of the daytime. Again, these results indicate that the AIRS V6 emissivity is less capable of capturing emissivity diurnal variations at this site. To further demonstrate this issue, the day/night difference over the Sahara Desert (6.00°E, 31.00°N), the same location used by *Masiello et al*., 2013, was evaluated. The results (not shown) indicate that the AIRS V6 emissivity is (1) able to capture the diurnal variation for 8.31 μm from April to October 2007, but with about 60% overestimation of the diurnal variations, and (2) not able to capture the diurnal variations for 10.41 and 12.02 μm.

These results indicate that the AIRS V6 emissivity demonstrates a major advance in terms of the emissivity seasonal variations; no unrealistic seasonal variations at CRCS Dunhuang site are observed. However, the emissivity diurnal variations between the day/night emissivity (from the descending/ascending orbits) are not well characterized, indicating possible limitations of AIRS V6 emissivity products. Cloud contamination is likely one of the major reasons for the limitation of AIRS emissivity products. Another possible and common difficulty in retrieving LSE is the residual effect from the algorithm for separating the LSE from the LST.

Figure 9 shows the long-term comparisons of monthly emissivity products for the MODIS 8.55 μm between the integrated UWIREMIS and the Terra/Aqua MODIS monthly products during 2007, together with two integrated field measurements. The V4.1 emissivities, both MOD and MYD, demonstrate a similar seasonal variation; the warm season has lower emissivities than the colder season. This variation is likely related to the soil moisture content, which is highly related to the surface skin temperature; higher temperature limits the soil moisture adsorption and thus resulting in lower emissivities. The V5 emissivities show no clear seasonal variations. The UWIREMIS follows the V4.1 trend very well because it is derived from the V4.1 MYD emissivity products.

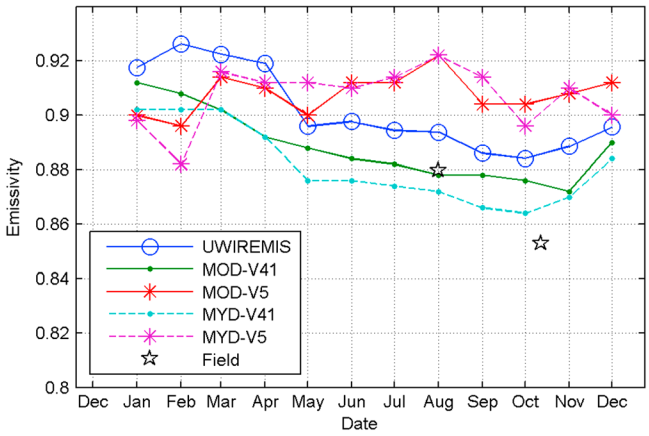

Figure 9. The time series of the 8.55 μm emissivity from the integrated UWIREMIS (blue circles), the V4.1 MOD (solid line with dots), and MYD (dashed line with dots) monthly products, and Version 5 (solid line with stars for MOD and dashed line with stars for MYD) for 2007. The integrated field measurements on 1 August and 12 October 2007 are also shown as individual black stars.

5. Discussions and Conclusions

Two sets of field-measured high spectral infrared emissivity spectra at the CRCS Dunhuang site were taken using a BOMEM MR154 Fourier transform spectroradiometer and Infrared Golden Board, one in the early morning (4–6 A.M. local time, representing night) on 1 August 2007 and the other in the afternoon (2–4 P.M. local time, representing day) on 12 October 2007. Comparing these two sets of emissivities reveals that the daytime emissivity is smaller than that at night in almost the entire spectrum between 7.5 and 14 μm. Based on our knowledge, these measurements are the first field measurements to support emissivity diurnal variations in a desert, which was first reported by *Z. Li et al.* [2012] and again by *Masiello et al.* [2013]. The basic reason for emissivity diurnal variation is that the evaporation from the sun heating the surface during the day reduces soil moisture, resulting in reduced emissivity, while at night increased adsorption of moisture by the sand particles increases soil moisture, resulting in increased emissivity.

These independent measurements are used to evaluate satellite-measured emissivity, including the UWIREMIS database, the operational AIRS level-3 emissivity products (Versions 5 and 6), and operational MODIS Terra/Aqua emissivity products (MOD11 and MYD11, Versions 4.1 and 5). Both 8 day and monthly products are examined. Time series of the different emissivity products are also studied. The results show the following:

1. AIRS, being a high spectral resolution IR sounder, has the high spectral resolving power critical for emissivity. However, due to the large footprint size, the radiance observations are more prone to cloud contamination, which may degrade the quality of the retrieved emissivity. Using the field measurements as a reference, the AIRS emissivity products are found to have poor quality at the CRCS Dunhuang site, with V6 having better quality than V5. The AIRS V6 emissivity products appear to have difficulty capturing the emissivity diurnal variations, which have been demonstrated by previous studies. One advantage of the hyperspectral IR sounder is its high resolving power of the high spectrum, although not demonstrated by AIRS. This makes applying the hyperspectral emissivity database friendlier.
2. A broadband IR imager, like MODIS, has the advantage of high spatial resolution and VIS/NIR channels to help the cloud mask, making the retrieval more reliable but with limited spectral bands. Using the field measurements as references, the V4.1 MODIS emissivity products are found to have better agreement than the AIRS emissivity products, the UWIREMIS and the V5 MODIS emissivity products at the CRCS Dunhuang site. The seasonal variation of MODIS V4.1 emissivity shows a reasonable pattern; emissivity in the warm seasons is lower than that of the cold seasons.
3. The UWIREMIS emissivity database takes advantages of both the high spatial resolution of MODIS and high spectral resolution from laboratory emissivity measurements and combines them. It should have a similar quality as the operational MODIS emissivity product. In this particular case, the UWIREMIS does not agree as well with the field measurements when compared with the MODIS V4.1 products but shows better agreement than the MODIS V5 and the AIRS emissivity products. More importantly, it is a high spectral resolution emissivity database, making it usable for all IR spectral bands, through convolving with spectral response functions.

One might consider combining the hyperspectral IR instrument with the high spatial resolution broadband IR instrument, taking advantage of both instruments to improve the emissivity retrieval. For example, one may use MODIS to help AIRS cloud detection, thus reducing the possibility of cloud contamination. However,

the chance for an AIRS footprint to be clear is less than 10% [*Hung-Lung and Smith*, 2004]. This will greatly limit the product yields. Another option is cloud clearing [*Li et al*., 2004; *Susskind et al*., 2003], which removes the cloud impacts and estimates the AIRS radiance by assuming that there are no clouds presented in a cloudy field of view. For retrieving emissivity, the cloud cleared radiances must have a quality similar to the clear observations, which no study has yet demonstrated.

Acknowledgments
The MODIS L3 emissivity data product was obtained through the online Data Pool at the NASA Land Processes Distributed Active Archive Center (LP DAAC), USGS/Earth Resources Observation and Science (EROS) Center, Sioux Falls, South Dakota (https://lpdaac.usgs.gov/data_access). The AIRS L3 emissivity data used in this study were acquired as part of the activities of NASA's Science Mission Directorate and are archived and distributed by the Goddard Earth Sciences (GES) Data and Information Services Center (DISC). The field emissivity spectra data were measured by Zhang et al. (zhangyong@cma.gov.cn) with a set of instruments at the CRCS Dunhuang site. The authors would like to thank the Cooperative Institute of Meteorological Satellite Studies (CIMSS) of the University of Wisconsin-Madison for providing the UWIREMIS database. The authors would also like to thank Lei Yang from the China Center for Resources Satellite Data and Application for providing GF-1 WFV data. This work is supported by Natural Science Foundation of China (grants 41171275 and 40701118) and the R&D Special Fund for Public Welfare Program (grant GYHY200906036).

References

Agam, N., and P. R. Berliner (2004), Diurnal water content changes in the bare soil of a coastal desert, *J. Hydrometeorol.*, *5*(5), 922–933, doi:10.1175/1525-7541(2004)005<0922:DWCCIT>2.0.CO;2.

BOMEM Inc. (1995), *The MR Series Documentation Set*, pp. 1–7, BOMEM Inc., Québec City.

Borbas, E., R. Knuteson, S. Seemann, E. Weisz, L. Moy, and H. Huang (2007), A high spectral resolution global land surface infrared emissivity database, Joint 2007 EUMETSAT Meteorological Satellite Conference and the 15th Satellite Meteorology and Oceanography Conference of the American Meteorological Society, Amsterdam, Netherlands, 24–28 Sept.

Capelle, V., A. Chédin, E. Péquignot, P. Schlüssel, S. M. Newman, and N. A. Scott (2012), Infrared continental surface emissivity spectra and skin temperature retrieved from IASI observations over the tropics, *J. Appl. Meteorol. Climatol.*, *51*, 1164–1179.

Chahine, M. T., et al. (2006), AIRS: Improving weather forecasting and providing new data on greenhouse gases, *Bull. Am. Meteorol. Soc.*, *87*, 991–926.

Clerbaux, C., J. Hadji-Lazaro, S. Turquety, G. Mégie, and P.-F. Coheur (2003), Trace gas measurements from infrared satellite for chemistry and climate applications, *Atmos. Chem. Phys. Discuss.*, *3*, 2027–2058, doi:10.5194/acpd-3-2027-2003.

Dong, L., J. Hu, S. Tang, and M. Min (2013), Field validation of the GLASS land surface broadband emissivity database using pseudo-invariant sand dune sites in northern China, *Int. J. Digital Earth*, doi:10.1080/17538947.2013.822573.

Faysash, A., and E. A. Smith (1999), Simultaneous land surface temperature-emissivity retrieval in the infrared split window, *J. Atmos. Oceanic Technol.*, *16*(11), 1673–1689, doi:10.1175/1520-0426(1999)016<1673:SLSTER>2.0.CO;2.

Faysash, A., and E. A. Smith (2000), Simultaneous retrieval of diurnal to seasonal surface temperatures and emissivities over SGP ARM-CART site using GOES split window, *J. Appl. Meteorol.*, *39*(7), 971–982, doi:10.1175/1520-0450(2000)039<0971:SRODTS>2.0.CO;2.

Galve, J., C. Coll, V. Caselles, and E. Valor (2008), An atmospheric radiosounding database for generating land surface temperature algorithms, *IEEE Trans. Geosci. Remote Sens.*, *46*(5), 1547–1557, doi:10.1109/TGRS.2008.916084.

Gillespie, A., S. Rokugawa, S. Hook, T. Matsunaga, and A. Kahle (1999), Temperature/emissivity separation algorithm theoretical basis document, version 2.4, report, NASA Goddard Space Flight Cent., Greenbelt, Md. [Available at http://eospso.gsfc.nasa.gov/eos_homepage/for_scientists/atbd/docs/ASTER/atbd-ast-05-08.pdf.]

Han, Y., et al. (2013), Suomi NPP CrIS measurements, sensor data record algorithm, calibration and validation activities, and record data quality, *J. Geophys. Res. Atmos.*, *118*, 12,734–12,748, doi:10.1002/2013JD020344.

Hapke, B. (1993), *Introduction to the Theory of Reflectance and Emittance Spectroscopy*, Cambridge Univ. Press, New York.

Hilton, F., et al. (2012), Hyperspectral Earth observation from IASI: Five years of accomplishments, *Bull. Am. Meteorol. Soc.*, *93*(3), 347–370, doi:10.1175/BAMS-D-11-00027.1.

Ho, S. P., D. P. Edwards, J. C. Gille, J. M. Chen, D. Ziskin, G. L. Francis, M. N. Deeter, and J. R. Drummond (2005), Estimates of 4.7 μm surface emissivity and their impact on the retrieval of tropospheric carbon monoxide by Measurements of Pollution in the Troposphere (MOPITT), *J. Geophys. Res.*, *110*, D21308, doi:10.1029/2005JD005946.

Hook, S., and A. Gabell (1992), Comparison of techniques for extracting emissivity information from thermal infrared data for geological studies, *Remote Sens. Environ.*, *42*, 123–135.

Hu, X., J. Liu, L. Sun, Z. Rong, Y. Li, Y. Zhang, Z. Zhao, R. Wu, L. Zhang, and X. Gu (2010), Characterization of CRCS Dunhuang test site and vicarious calibration utilization for Fengyun (FY) series sensors, *Can. J. Remote Sens.*, *36*(5), 566–582.

Hulley, G., and S. Hook (2009a), The North American ASTER Land Surface Emissivity Database (NAALSED) Version 2.0, *Remote Sens. Environ.*, *113*(9), 1967–1975, doi:10.1016/j.rse.2009.05.005.

Hulley, G., and S. Hook (2009b), Intercomparison of versions 4, 4.1 and 5 of the MODIS Land Surface Temperature and Emissivity products and validation with laboratory measurements of sand samples from the Namib Desert, Namibia, *Remote Sens. Environ.*, *113*(6), 1313–1318.

Hulley, G., S. Hook, and A. M. Baldridge (2010), Investigating the effects of soil moisture on thermal infrared land surface temperature and emissivity using satellite retrievals and laboratory measurements, *Remote Sens. Environ.*, *114*, 1480–1493, doi:10.1016/j.rse.2010.02.002.

Hung-Lung, H., and W. L. Smith (2004), Apperception of clouds in AIRS data, in *Proceedings ECMWF Workshop on Assimilation of High Spectral Resolution Sounders in NWP*, pp. 155–169, Reading, U. K., 28 June-1 July.

Ingram, P., and M. Henry (2001), Sensitivity of iterative spectrally smooth temperature/emissivity separation to algorithmic assumptions and measurement noise, *IEEE Trans. Geosci. Remote Sens.*, *39*(10), 2158–2167.

Jackson, T., P. O'Neill, and C. Swift (1997), Passive microwave observation of diurnal surface soil moisture, *IEEE Trans. Geosci. Remote Sens.*, *35*(5), 1210–1222, doi:10.1109/36.628788.

Jacob, F., F. Petitcolin, T. Schmugge, E. Vermote, K. Ogawa, and A. French (2004), Comparison of land surface emissivity and radiometric temperature from MODIS and ASTER sensors, *Remote Sens. Environ.*, *83*, 1–18.

Le Marshall, J., et al. (2006), Improving global analysis and forecasting with AIRS, *Bull. Am. Meteorol. Soc.*, *87*, 891–894, doi:10.1175/BAMS-87-7-891.

Lee, H.-T., A. Gruber, R. G. Ellingson, and I. Laszlo (2007), Development of the HIRS outgoing longwave radiation climate data set, *J. Atmos. Oceanic Technol.*, *24*, 2029–2047, doi:10.1175/2007JTECHA989.1.

Li, J., and J. Li (2008), Derivation of global hyperspectral resolution surface emissivity spectra from advanced infrared sounder radiance measurements, *Geophys. Res. Lett.*, *35*, L15807, doi:10.1029/2008GL034559.

Li, J., W. P. Menzel, F. Sun, T. J. Schmit, and J. Gurka (2004), AIRS subpixel cloud characterization using MODIS cloud products, *J. Appl. Meteorol.*, *43*, 1083–1094.

Li, J., H. Huang, C. Liu, P. Yang, T. Schmit, H. Wei, E. Weisz, L. Guan, and W. Menzel (2005), Retrieval of cloud microphyiscal properties from MODIS and AIRS, *J. Appl. Meteorol.*, *44*, 1526–1543, doi:10.1175/JAM2281.1.

Li, J., P. Zhang, T. J. Schmit, J. Schmetz, and W. P. Menzel (2007a), Quantitative monitoring of a Saharan dust event with SEVIRI on Meteosat-8, *Int. J. Remote Sens.*, *28*, 2181–2186, doi:10.1080/01431160600975337.

Li, J., J. Li, E. Weisz, and D. K. Zhou (2007b), Physical retrieval of surface emissivity spectrum from hyperspectral infrared radiances, *Geophys. Res. Lett.*, *34*, L16812, doi:10.1029/2007GL030543.
Li, J., Z. Li, X. Jin, T. J. Schmit, L. Zhou, and M. D. Goldberg (2011), Land surface emissivity from high temporal resolution geostationary infrared imager radiances: Methodology and simulation studies, *J. Geophys. Res.*, *116*, D01304, doi:10.1029/2010JD014637.
Li, Z., J. Li, W. P. Menzel, T. J. Schmit, J. P. Nelson III, J. Daniels, and S. A. Ackerman (2008), GOES sounding improvement and applications to severe storm nowcasting, *Geophys. Res. Lett.*, *35*, L03806, doi:10.1029/2007GL032797.
Li, Z., J. Li, W. P. Menzel, J. P. Nelson III, T. J. Schmit, E. Weisz, and S. A. Ackerman (2009), Forecasting and nowcasting improvement in cloudy regions with high temporal GOES sounder infrared radiance measurements, *J. Geophys. Res.*, *114*, D09216, doi:10.1029/2008JD010596.
Li, Z., J. Li, X. Jin, T. J. Schmit, E. E. Borbas, and M. D. Goldberg (2010), An objective methodology for infrared land surface emissivity evaluation, *J. Geophys. Res.*, *115*, D22308, doi:10.1029/2010JD014249.
Li, Z., J. Li, Y. Li, Y. Zhang, T. J. Schmit, L. Zhou, M. D. Goldberg, and W. P. Menzel (2012), Determining diurnal variations of land surface emissivity from geostationary satellites, *J. Geophys. Res.*, *117*, D23302, doi:10.1029/2012JD018279.
Li, Z. L., H. Wu, N. Wang, S. Qiu, J. Sobrino, Z. Wan, B. Tang, and G. Yan (2012), Land surface emissivity retrieval from satellite data, *Int. J. Remote Sens.*, *34*(9–10), 3084–3127.
Masiello, G., C. Serio, S. Venafra, I. Defeis, and E. Borbas (2013), Diurnal variation in Sahara desert sand emissivity during the dry season from IASI observations, *J. Geophys. Res. Atmos.*, *119*, 1626–1638, doi:10.1002/jgrd.50863.
Menzel, W., R. Frey, H. Zhang, D. Wylie, C. Moeller, R. Holz, B. Maddux, B. Baum, K. Strabala, and L. Gumley (2008), MODIS global cloud-top pressure and amount estimation: Algorithm description and results, *J. Appl. Meteorol. Climatol.*, *47*(4), 1175–1198, doi:10.1175/2007JAMC1705.1.
Mira, M., E. Valor, R. Boluda, V. Caselles, and C. Coll (2007), Influence of soil water content on the thermal infrared emissivity of bare soils: Implication for land surface temperature determination, *J. Geophys. Res.*, *112*, F04003, doi:10.1029/2007JF000749.
Morgan, J. A. (2005), Bayesian estimation for land surface temperature retrieval: The nuisance of emissivities, *IEEE Trans. Geosci. Remote Sens.*, *43*(6), 1279–1288, doi:10.1109/TGRS.2005.845637.
Nerry, F., J. Labed, and M.-P. Stoll (1988), Emissivity signatures in the thermal IR band for remote sensing: Calibration procedure and method of measurement, *Appl. Opt.*, *27*, doi:10.1364/AO.27.000758.
Nerry, F., J. Labed, and M. P. Stoll (1990), Spectral properties of land surfaces in the thermal infrared: 1. Laboratory measurements of absolute spectral emissivity signatures, *J. Geophys. Res.*, *95*(B5), 7027–7044.
Ogawa, K., T. Schmugge, and S. Rokugawa (2006), Observations of the dependence of the thermal infrared emissivity on soil moisture, *Geophys. Res. Abstr.*, *8*, 04996.
Pavelin, E. G., and B. Candy (2014), Assimilation of surface-sensitive infrared radiances over land: Estimation of land surface temperature and emissivity, *Q. J. R. Meteorol. Soc.*, *140*, 1198–1208, doi:10.1002/qj.2218.
Peres, L. F., and C. C. DaCamara (2004), Land surface temperature and emissivity estimation based on the two-temperature method: Sensitivity analysis using simulated MSG/SEVIRI data, *Remote Sens. Environ.*, *91*, 377–389, doi:10.1016/j.rse.2004.03.011.
Rees, W. G., and S. P. James (1992), Angular variation of the infrared emissivity of ice and water surfaces, *Int. J. Remote Sens.*, *13*(15), 2873–2886.
Rodger, A. P., L. K. Balick, and W. B. Clodius (2005), The performance of the Multispectral Thermal Imager (MTI) surface temperature retrieval algorithm at three sites, *IEEE Trans. Geosci. Remote Sens.*, *43*(3), 658–665, doi:10.1109/TGRS.2004.840642.
Rubio, E., V. Caselles, and C. Badenas (1997), Emissivity measurements of several soils and vegetation types in the 8 ~ 14 μm wave band: Analysis of two field methods, *Remote Sens. Environ.*, *59*, 490–521.
Ruston, B., F. Z. Weng, and B. H. Yan (2008), Use of a one-dimensional variational retrieval to diagnose estimates of infrared and microwave surface emissivity over land for ATOVS sounding instruments, *IEEE Trans. Geosci. Remote Sens.*, *46*(2), 393–402.
Salisbury, J., and D. Aria (1992), Emissivity of terrestrial materials in the 8–14 μm atmospheric windows, *Remote Sens. Environ.*, *42*, 83–106.
Sanchez, J. M., A. N. French, and M. Mira (2011), Thermal infrared emissivity dependence on soil moisture in field conditions, *IEEE Trans. Geosci. Remote Sens.*, *49*(11), 4652–4659.
Schmetz, J., P. Pili, S. Tjemkes, D. Just, J. Kerkman, S. Rota, and A. Ratier (2002), An introduction to Meteosat Second Generation (MSG), *Bull. Am. Meteorol. Soc.*, *83*(7), 977–992, doi:10.1175/1520-0477(2002)083<0977:AITMSG>2.3.CO;2.
Schmit, T. J., M. M. Gunshor, W. Paul Menzel, J. Gurka, J. Li, and S. Bachmeier (2005), Introducing the next-generation advanced baseline imager (ABI) on GOES-R, *Bull. Am. Meteorol. Soc.*, *86*, 1079–1096.
Schmugge, T., and K. Ogawa (2006), Validation of emissivity estimates from ASTER and MODIS data, in *Proceeding of Geoscience and Remote Sensing Symposium*, pp. 260–262, New Mexico State Univ., Las Cruces, N. M., doi:10.1109/IGARSS.2006.71.
Seemann, S. W., E. E. Borbas, R. O. Knuteson, G. R. Stephenson, and H.-L. Huang (2008), Development of a global infrared land surface emissivity database for application to clear sky sounding retrievals from multi-spectral satellite radiance measurements, *J. Appl. Meteorol. Climatol.*, *47*, 108–123.
Sobrino, J. A., N. Raissouni, and Z. L. Li (2001), A comparative study of land surface emissivity retrieval from NOAA Data, *Remote Sens. Environ.*, *75*(2), 256–266, doi:10.1016/S0034-4257(00)00171-1.
Susskind, J., J. M. Blaisdell, and L. Iredell (2014), Improved methodology for surface and atmospheric soundings, error estimates, and quality control procedures: The atmospheric infrared sounder science team version-6 retrieval algorithm, *J. Appl. Remote Sens.*, *8*(1), 084994, doi:10.1117/1.JRS.8.084994.
Susskind, J., C. D. Barnet, and J. M. Blaisdell (2003), Retrieval of atmospheric and surface parameters from AIRS/AMSU/HSB data in the presence of clouds, *IEEE Trans. Geosci. Remote Sens.*, *41*, 390–409.
Tian, B., E. Manning, E. Fetzer, E. Olsen, W. Sun, J. Susskind, and L. Iredell (2013), AIRS/AMSU/HSB version 6 level 3 product user guide, Jet Propul. Lab., Calif. Insti. Tech.
Wan, Z. (2014), New refinements and validation of the collection-6 MODIS land-surface temperature/emissivity product, *Remote Sens. Environ.*, *140*, 36–45, doi:10.1016/j.rse.2013.08.027.
Wan, Z., and Z.-L. Li (1997), A physics-based algorithm for retrieving land surface emissivity and temperature from EOS/MODIS data, *IEEE Trans. Geosci. Remote Sens.*, *35*(4), 980–996.
Wan, Z., Y. Zhang, X. Ma, M. D. King, J. S. Myers, and X. Li (1999), Vicarious calibration of the Moderate-Resolution Imaging Spectroradiometer Airborne Simulator thermal infrared channels, *Appl. Opt.*, *38*(20), 6294–6306.
Wan, Z., Y. Zhang, Z. Li, R. Wang, V. Salomonson, A. Yves, R. Bosseno, and J. Hanocq (2002), Preliminary estimate of calibration of the moderate resolution imaging spectroradiometer thermal infrared data using Lake Titicaca, *Remote Sens. Environ.*, *80*(3), 497–515.
Wan, Z. M. (2008), New refinements and validation of the MODIS land-surface temperature/emissivity products, *Remote Sens. Environ.*, *112*, 59–74.
Watson, K. (1992), Two-temperature method for measuring emissivity, *Remote Sens. Environ.*, *42*, 117–121, doi:10.1016/0034-4257(92)90095-2.

Zhang, P., N. Lu, X. Hu, and C. H. Dong (2006), Identification and physical retrieval of dust storm using three MODIS thermal IR, *Global Planet. Change*, *52*, 197–206, doi:10.1016/j.gloplacha.2006.02.014.

Zhang, R. H. (1999), Some thinking on quantitative thermal infrared remote sensing, *Remote Sens. Land Resour.*, *39*(1), 1–6.

Zhang, R. H., and G. L. Tian (1981), Measurement of objects emissivity at room temperature, *Chin. Sci. Bull.*, *5*, 297–300.

Zhang, Y. (2012), Technical report of Fengyun Satellites infrared channels radiometric calibration of 2012 CRCS experimentations, National Satellite Meteorological Center, *Tech. Note*, 1–10 Nov.

Zhang, Y., and C. Qi (2013), Technical report of Fengyun Satellites infrared channels radiometric calibration of 2013 CRCS experimentations, National Satellite Meteorological Center, *Tech. Note*, 1–16 Dec. 2013.

Zhang, Y., X. Gu, T. Yu, Y. Zhang, L. Cheng, X. Y. Li, X. Li, and L. He (2005), Absolute radiometric calibration of CBERS-02 IRMSS thermal band, *Sci. China, Ser. E: Eng. Mater. Sci.*, *48*(Supp.I), 72–90.

Zhang, Y., Y. Li, Z. Rong, X. Hu, L. Zhang, and J. Liu (2009a), Field measurement of Gobi surface emissivity spectrum at Dunhuang calibration site of China, *Spectrosc. Spectral Anal.*, *29*(5), 12131217.

Zhang, Y., H. Yang, Z. J. Zheng, L. J. Zhang, Q. F. Lu, G. C. Li, and Z. D. Yang (2009b), Field measurements of meadow surface emissivity spectra at the Xilinhaote grassland of China, *Acta Prataculturae Sin.*, *18*(5), 31–39.

Zhang, Y., Z. Zheng, X. Hu, Z. Rong, and L. Zhang (2013), Lake Qinghai: Chinese site for radiometric calibration of satellite infrared remote sensors, *Remote Sens. Lett.*, *4*(4), 315–324.

Zhao, Y., et al. (2003), *The Principle and Method of Analysis of Remote Sensing Application*, Science Press, Beijing.

Zhou, L., M. Goldberg, C. Barnet, Z. Cheng, F. Sun, W. Wolf, T. King, X. Liu, H. Sun, and M. Divakarla (2008), Regression of surface spectral emissivity from hyperspectral instruments, *IEEE Trans. Geosci. Remote Sens.*, *46*, 328–333, doi:10.1109/TGRS.2007.912712.